JOURNAL OF VIROLOGY, June 2009, p. 6234–6246 Vol. 83, No. 12
0022-538X/09/$08.00+0 doi:10.1128/JVI.00282-09

Simultaneous Cell-to-Cell Transmission of Human Immunodeficiency Virus to Multiple Targets through Polysynapses▽†

Dominika Rudnicka,[1] Jérôme Feldmann,[1] Françoise Porrot,[1] Steve Wietgrefe,[2] Stéphanie Guadagnini,[3] Marie-Christine Prévost,[3] Jérôme Estaquier,[4] Ashley T. Haase,[2] Nathalie Sol-Foulon,[1]*‡ and Olivier Schwartz[1]*‡

Virus and Immunity Unit, Department of Virology, Institut Pasteur, URA CNRS 3015, 28 rue du Dr. Roux, 75724 Paris Cedex 15, France[1]; Department of Microbiology, University of Minnesota Medical School, MMC 196, 420 Delaware Street Southeast, Minneapolis, Minnesota 55455[2]; Electron Microscopy Core Facility, Institut Pasteur, Paris, France[3]; and INSERM U841, Faculté de Médecine Henri Mondor, 8 rue du Général Sarrail, 94010 Créteil, France[4]

Received 9 February 2009/Accepted 2 April 2009

Human immunodeficiency virus type 1 (HIV-1) efficiently propagates through cell-to-cell contacts, which include virological synapses (VS), filopodia, and nanotubes. Here, we quantified and characterized further these diverse modes of contact in lymphocytes. We report that viral transmission mainly occurs across VS and through "polysynapses," a rosette-like structure formed between one infected cell and multiple adjacent recipients. Polysynapses are characterized by simultaneous HIV clustering and transfer at multiple membrane regions. HIV Gag proteins often adopt a ring-like supramolecular organization at sites of intercellular contacts and colocalize with CD63 tetraspanin and raft components GM1, Thy-1, and CD59. In donor cells engaged in polysynapses, there is no preferential accumulation of Gag proteins at contact sites facing the microtubule organizing center. The LFA-1 adhesion molecule, known to facilitate viral replication, enhances formation of polysynapses. Altogether, our results reveal an underestimated mode of viral transfer through polysynapses. In HIV-infected individuals, these structures, by promoting concomitant infection of multiple targets in the vicinity of infected cells, may facilitate exponential viral growth and escape from immune responses.

Human immunodeficiency virus type 1 (HIV-1) and simian immunodeficiency virus (SIV) mostly replicate in $CD4^+$ memory T cells throughout the lymphoid tissues. A compartmentalization of HIV-1 quasispecies, associated with the presence of multiply infected cells, has been observed in microdissected splenic germinal centers (12), suggesting that viral dissemination occurs by local replication in nearby cells. Viral spread is driven by cell-free virions and, in a much more efficient and rapid way, through direct transfer of infection across cell-to-cell contacts (41, 44). Various modes of cell-to-cell HIV transfer in culture have been reported (1, 11, 13, 22, 33, 46, 49, 50). For instance, HIV-1 readily forms virological synapses (VS) at the interface between HIV-infected cells and targets (44). VS were initially described by Bangham et al., to characterize human T-cell leukemia virus type 1 (HTLV-1) transfer in lymphocytes (20). The HIV-1 or HTLV-1 VS represents a polarized accumulation of viruses at the contact zone between one individual infected cell and one target. Regarding HIV-1, VS formation involves HIV Env-CD4-coreceptor interactions and requires cytoskeletal rearrangements and stabilization of cell junctions by adhesion molecules (3, 22–24). Interestingly, the VS likely allows HIV to evade antibody neutralization (3), although Env-independent mechanisms of viral transfer have been reported (11, 21). Interestingly, HIV dissemination through VS involves viral endocytosis in target cells (18, 43). Another mode of retroviral transfer involves the establishment of filopodial bridges (or viral cytonemes) between infected cells and targets (46). Viruses move along the outer surface of the bridge toward the target cell, in a kind of stretched-out VS (17). More recently, thinner structures called membrane nanotubes, which form when cells make contact and subsequently part, have been reported to mediate HIV spread (7, 50). Both filopodia and nanotubes might allow transfer to distant cells, as observed not only with retroviruses, but also with numerous viral species, like herpesvirus, papillomavirus, and vaccinia virus (5, 28, 34, 45, 47). Limiting cell contacts by gently agitating cells significantly reduces HIV spread in culture (49), but the relative contributions of VS, filopodia, and nanotubes to viral replication remain poorly understood.

Here, we investigated HIV spread in $CD4^+$ lymphocytes by combining diverse techniques of visualization (three-dimensional [3D] reconstructions of confocal immunofluorescence [IF], scanning electron microscopy [SEM], correlative IF-transmission electron microscopy [TEM], and real-time imaging of HIV Gag movements). We quantified the frequency of VS, filopodia, and nanotubes in culture. We identified in lymphocytes a poorly characterized structure of viral transmission that we termed "polysynapse," in which one infected cell simultaneously transfers the virus to multiple adjacent recipi-

* Corresponding author. Mailing address: Virus and Immunity Unit, Department of Virology, Institut Pasteur, URA CNRS 3015, 28 rue du Dr. Roux, 75724 Paris Cedex 15, France. Phone for N.S.-F.: 331 45688783. Fax: 331 40613465. E-mail: natsol@pasteur.fr. Phone for O.S.: Phone: 331 45688353. Fax: 331 40613465. E-mail: schwartz@pasteur.fr.

† Supplemental material for this article may be found at http://jvi.asm.org/.

‡ N.S.-F. and O.S. contributed equally to this work.

▽ Published ahead of print on 15 April 2009.

ents. We further describe some cellular and viral mechanisms involved in the formation of polysynapses.

MATERIALS AND METHODS

Cells and viruses. Jurkat cells, Jβ2.7 cells, phytohemagglutinin-activated human primary CD4 T lymphocytes, or monocyte-derived dendritic cells (DCs) were infected with HIV [NL4-3 for lymphocytes, NL4-3(VSV) pseudotypes for DCs] or a Δ*env* mutant derivative as described previously (48, 49). Jurkat derivative Jβ2.7 cells (which lack LFA-1) and Jβ2.7-LFA1$^+$ cells (in which LFA-1 expression was restored) were a kind gift from Catarina Hioe (15). Cells were used 2 to 3 days postinfection, when 25 to 80% of T cells and 20 to 40% of DCs were Gag$^+$. Production and use of the HIV construct (Gag-eGFP) carrying enhanced green fluorescent protein (EGFP) (36) are described in the supplemental material. HIV replication was assessed by measuring the percentage of Gag$^+$ cells over time as described previously (48, 49).

IF analysis. For IF analysis, HIV-infected donor cells were mixed with target cells (prelabeled with CellTrace Far Red DDAO-SE; Molecular Probes) at a 1/1 ratio and loaded onto polylysine-coated coverslips (1×10^6cells in 350 μl). After 1 h at 37°C, cells were fixed and analyzed as described in the supplemental material.

Inhibitors of actin and tubulin remodeling. HIV-infected donor cells were treated with either nocodazole (1 μM; Calbiochem) or cytochalasin D or latrunculin B (1 μM each; Sigma) for 1 h at 37°C prior to mixing with targets as described previously (24). The compounds induced the expected inhibitory effects on tubulin (nocodazole) and actin (cytochalasin D or latrunculin B) cytoskeletons, as observed by IF (not shown).

Quantification of cell conjugates. Quantification of various types of cell-cell contact was performed by visual observation of multiple low-power fields, directly at the microscope or after image acquisition. The total number of infected cells was counted. Cell conjugates were defined as pairs (single conjugates) or groups of cells (multiple conjugates) closely apposed, among which at least one donor was Gag$^+$. Cells with filopodia or nanotubes were similarly scored. The percentage of infected cells with a capping of Gag at the junction sites with targets was scored by visual examination.

Analysis of HIV cell-to-cell transfer and of HIV replication by flow cytometry. Donor cells were infected with HIV NL4-3 and used a few days later, when 25% of the cells were Gag$^+$. Cell-to-cell HIV transfer was performed as described previously (48, 49). Target cells were labeled with carboxyfluorescein succinimidyl ester (CFSE; 2.5 μM) (Molecular Probes) for 10 min at 37°C. Donor and target cells were then mixed at the indicated ratio, in 24-well plates, at a final concentration of 1×10^6/ml in a final volume of 200 μl. At the indicated time points, cells were fixed in 2% paraformaldehyde, permeabilized with phosphate-buffered saline–1% bovine serum albumin–0.05% saponin and stained for intracellular Gag using anti-p24^{gag} RD1-coupled monoclonal antibody (MAb) KC57 (Coulter) and analyzed by flow cytometry. For HIV replication studies, the fraction of Gag$^+$ cells was similarly measured by flow cytometry.

The techniques used for electron microscopy, correlative IF-TEM, and live imaging of HIV-infected cells are described in the supplemental material.

Analysis of lymphoid tissues from SIV-infected macaques. SIV RNA$^+$ cells were detected after reexamination of samples from SIV-infected macaques from a previous study (54) as described in the supplemental material.

RESULTS

Qualitative and quantitative analysis of HIV cell-to-cell spread. We first examined how HIV-1-infected T cells interact with noninfected targets. To this end, productively infected Jurkat cells (Fig. 1a and b) or primary CD4$^+$ lymphocytes (Fig. 1c and d) were mixed with Far Red dye-labeled recipients. After 1 h of coculture, the presence of cell conjugates, the type of contacts, and the accumulation of HIV Gag proteins were visualized by IF and quantified. Three main types of contacts were detected and scored (Fig. 1). Tight clusters between one individual donor and one recipient, associated with a large accumulation of Gag proteins at the contact zone, a hallmark of VS (20, 22), occurred in about 25% of cases (Fig. 1). Remote contacts, with actin-positive structures reminiscent of filopodial bridges or tunneling nanotubes (46, 50), were observed in <10% of infected cells. A punctate Gag signal was readily visible on these membrane extensions, likely corresponding to virions transiting toward targets. Finally, a significant fraction of HIV-infected cells (15% and 20% in Jurkat and primary CD4$^+$ T cells, respectively) was engaged, through close contacts, with two to six uninfected targets at a time (Fig. 1). Within these groups of cells, a Gag signal concentrating at each zone of engagement was detected in the donor (in 35% of Jurkat or primary CD4$^+$ cells, Fig. 1), whereas more than one target displayed Gag-positive dots. This strongly suggests that a single infected cell may simultaneously transmit infection to multiple recipients. We refer to this superposition of Gag clusters as a "polysynapse."

The number of conjugates between HIV-infected donors and targets was twofold higher than with uninfected donors in both Jurkat and primary CD4$^+$ T cells (Fig. 1), confirming that infection enhanced or stabilized lymphocyte interactions (3, 22). This was also the case with filopodia- or nanotube-like structures, which were enhanced upon HIV infection (Fig. 1). The number of cells with polarized Gag, within single or multiple conjugates, was decreased when donor cells expressed noninfectious envelope (gp120)-deleted HIV (Fig. 1) or when CD4-negative lymphocytes were used as targets (not shown). Thus, as for single VS (22), polysynapses required cognate HIV envelope-receptor interactions. It is noteworthy that in the experiments depicted above, we used a donor/target ratio of 1:1. Increasing the number of donor Jurkat cells induced an augmentation of the total number of synapses without obvious changes in the ratio of mono- versus polysynapses (not shown). We also mixed infected donor and target Jurkat cells at +4°C for 1 h. At this temperature, the numbers of conjugates and mono- and polysynapses were dramatically decreased (not shown), suggesting that synapse formation is an active process.

Altogether, these results indicate that in our cocultures of infected lymphocytes and recipients, various modes of cell interactions and viral transfer can be observed at the same time. Tight interactions through synapses are the most frequent modes of contact. Infected cells readily form polysynapses, associating with multiple targets. Remote interactions through filopodia or nanotube like structures are less frequently detected.

A ring-like structure of Gag proteins at the synapse. Strikingly, 3D *z*-stack reconstructions revealed a previously undescribed ring pattern of Gag at the site of cell-cell contact (Fig. 2; and see Movie S1 in the supplemental material). This ring of Gag proteins occurred in cells engaged in single VS and in polysynapses (Fig. 2; and see Movie S1 in the supplemental material). Examples of conjugates harboring or not harboring a Gag ring are depicted in Fig. 2a and b. It is noteworthy that the presence of one or more rings of Gag proteins was observed in 44% and 67% of cells displaying VS and polysynapses, respectively (34 VS and 113 polysynapses analyzed). The ring distribution was not due to an artifact of staining with anti-Gag antibodies, since it was also observed with an infectious HIV strain carrying a Gag-GFP fusion protein (GFP localization in Fig. 2c). Thus, upon cellular contact, viral proteins often accumulate at the periphery of the junction zone and adopt a structure reminiscent of pSMAC of adhesion molecules observed in immunological synapses (6).

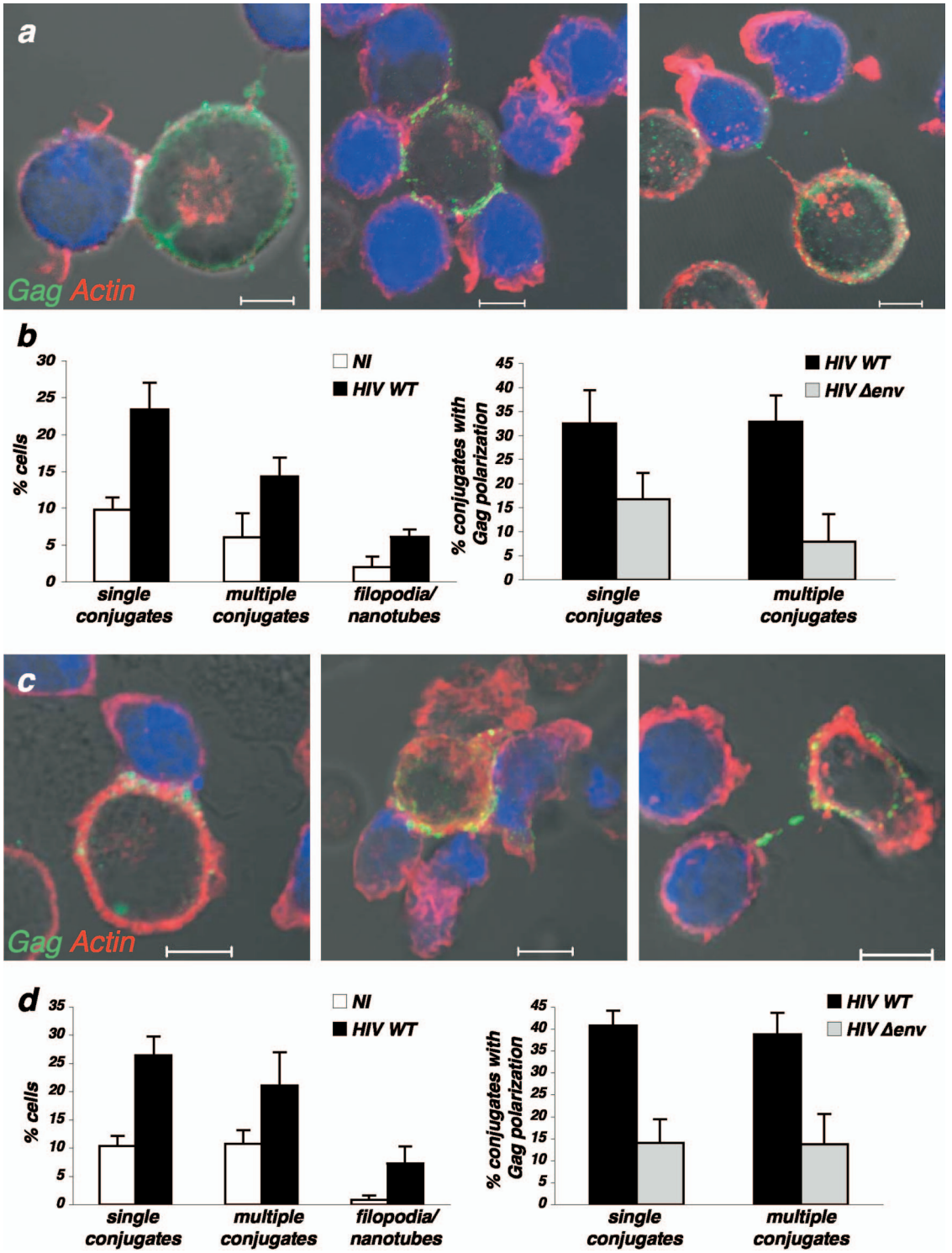

FIG. 1. Distinct modes of contact between HIV-1-infected cells and targets. (a and b) Jurkat cells; (c and d) primary $CD4^+$ T cells. (a and c) Confocal images illustrating classical virological synapses (left), polysynapses (middle), and remote contacts through filopodial bridges or nanotube-like structures (right). HIV-1-infected cells were mixed with Far Red dye-labeled recipients (blue) for 1 h and stained for HIV-1 Gag (green) and F-actin (red). The scale bar represents 5 μm. (a) Jurkat cells; (c) primary $CD4^+$ T cells. (b and d) Quantification of the various types of contacts. (Left) Noninfected (NI) or HIV-1-infected cells were cocultivated with targets, and the indicated types of contacts were scored. (Right) Quantification of HIV-infected cells (HIV wild type [WT] or Δ*env* mutant) displaying Gag clustering at the junction zone with targets. Data are means ± standard deviations of four independent experiments. A total of 1,685 NI cells and 1,247 WT HIV- and 1,137 Δ*env*-mutant-infected Jurkat cells were analyzed in panel b, and 1,646 NI cells and 693 WT HIV- and 522 Δ*env* mutant-infected primary $CD4^+$ T cells were analyzed in panel d.

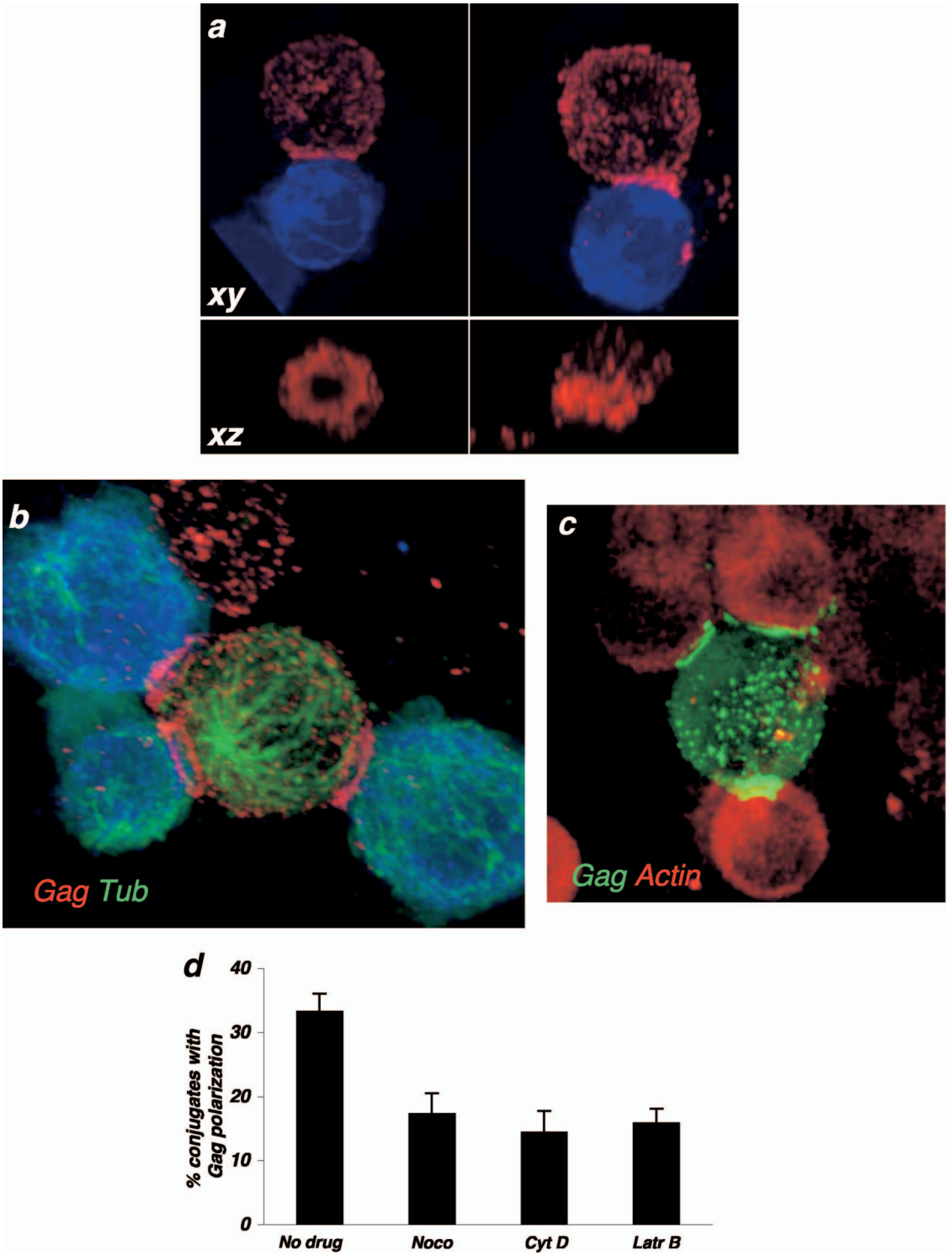

FIG. 2. Characteristics of virological polysynapses. Conjugates between infected cells and targets (blue) were stained with anti-Gag (a) or with anti-Gag and antitubulin (Gag Tub) (b). (a) Representative images of single synapses, in which Gag proteins adopt (left panel) or do not adopt (right panel) a ring-like structure at the junction zone. A magnification of the junction, on the *xz* axis, is shown in the lower panels. (b) Example of a polysynapse, with a single donor interacting simultaneously with three targets. The image is a snapshot from movie S1 in the supplemental material. (c) Example of a polysynapse, between one cell infected with an infectious HIV strain carrying a Gag-GFP fusion protein and targets harboring an actin-RFP fusion. Gag localization is revealed by GFP. (d) Effects of inhibitors of actin (1 μM each cytochalasin D [Cyt D] and latrunculin B [Latr B]) and microtubule (1 μM nocodazole [Noco]) remodeling on the recruitment of Gag at polysynapses. Data are means ± standard deviations of three independent experiments (with 604 to 1,232 infected cells analyzed, depending on the treatment).

Characteristics of virological polysynapses. We further characterized the structural organization of polysynapses. We first examined the localization of the microtubule organizing center (MTOC) and of a panel of cellular proteins. There was no preferential Gag accumulation at plasma membrane subdomains facing the MTOC (Fig. 2b; and see Movie S1 in the supplemental material). The actin and tubulin cytoskeletons control Gag and Env trafficking and assembly in GM1-enriched platforms, as well as VS constitution (3, 24, 31, 39). Inhibitors of actin (cytochalasin D or latrunculin B) and tubulin (nocodazole) remodeling decreased the number of polysynapses by 50% (Fig. 2d). As expected (3, 24), these compounds did not reduce the number of contacts between infected cells and target cells and inhibited to a similar extent classical VS (not shown). Therefore, formation of both single VS and polysynapses involves dynamic movements of the cytoskeleton.

We observed frequent enrichment of the raft marker GM1 and the tetraspanin CD63 in the polysynaptic structures (Fig. 3). We then investigated the distribution of Thy-1 and CD59, two glycosylphosphatidylinositol-linked proteins that partition into lipid rafts (38). Thy-1 and CD59 were also preferentially distributed at the contact zone between infected cells and targets (Fig. 3). Of note, GM-1, as well as CD63, Thy-1, CD59, and Env, often adopted a ring-like distribution and colocalized with Gag in polysynapses (not shown). Colocalization of Gag with Env, CD63, and GM1 in polysynapses, eventually in a ring distribution (not shown), was also observed in primary lymphocytes (see Fig. S1 in the supplemental material). Thus, as described for VS and for DC–T-cell transinfections (10, 25, 26), polysynapse formation potentially involves tetraspanins and lipid raft microdomains.

We next examined the localization of Env glycoproteins in Jurkat cells displaying polysynapses (Fig. 4a). Most of the Env signal appeared in a perinuclear region, likely corresponding to newly synthesized glycoproteins in the Golgi apparatus or the endosomal/recycling compartment. The cell surface was also faintly Env positive, with a more intense signal and a colocalization with Gag at sites of intercellular contacts. This suggested that infectious viruses were accumulating at these sites. HIV budding was then visualized by SEM analysis, combined with anti-Env immunogold staining. Virus-like particles, decorated with Env-positive dots, were observed at the surface of infected cells and not in naive cells (see Fig. S2 in the supplemental material). In cocultures, numerous Env^+ particles were found at the junction zone of donors and recipients (Fig. 4b).

It is noteworthy that SEM also revealed the presence of cells with long protrusions harboring Env^+ viral particles (Fig. 4c). Therefore, the filopodial-like structures observed by IF (Fig. 1) likely transport infectious viral particles.

We then used correlative IF-TEM in order to visualize viral budding and accumulation in polysynapses over a wide range of magnifications. A typical polysynapse, with a conjugate of one infected and three target cells, was first identified by IF (Fig. 5). As expected, Gag proteins were engaged at different zones of contact. This cluster was examined further by TEM after serial sectioning (Fig. 5). Three sections, separated by 0.5 to 1 μM (*z* axis) and corresponding, respectively, to the upper, middle, and lower regions of the conjugates, are depicted (Fig. 5). Numerous virions, at various stages of the release process, were detected at the junctions. Immature viral particles, budding from the infected cell or accumulating in the extracellular space, are present. Mature virions, detached from the producer cell and displaying a characteristic cone shape structure of the viral core, were detected in intercellular clefts as well as in zones of close junctions (see another example of a polysynapse analyzed by TEM in Fig. S3a in the supplemental material). These viral particles may have either budded locally or been transported through lateral movements at the plasma membrane. Virions were often bound to targets, strongly suggesting that they are in the process of entering and/or fusing with these cells. Interestingly, in some cases, virions were found at the periphery of the intercellular contacts, whereas the regions of tight membrane juxtaposition were devoid of viral material (Fig. 5). This organization may correspond to the rings of Gag proteins detected by IF and suggests that these rings originate from a preferential accumulation of virions at the periphery, rather than in the center of the synapse. In other cases, virions appear to bud at the contact zone (see Fig. S3a in the supplemental material), which is in line with our quantification of the Gag rings by IF, in about half of the synapses.

Altogether, the combined use of SEM and correlative microscopy indicates that the Gag and Env signals detected by IF in polysynapses correspond mostly to viral particles at various stages of budding, release, extracellular accumulation, and binding to targets.

Real-time imaging of HIV cell-to-cell transfer. We then assessed in living HIV-infected T cells the localization and trafficking of Gag toward polysynapses. To this end, we used a fluorescent virus carrying EGFP at the C terminus of the matrix domain of Gag (36). This virus, when coexpressed with wild-type HIV, remains infectious, albeit with reduced relative infectivity, and is a convenient tool to study the movements of HIV Gag proteins in donor cells (27, 36). HIV Gag.eGFP-infected Jurkat cells were cocultivated with target cells that expressed red fluorescent protein (RFP)-actin. Images were acquired every 30 s for up to 1 h. A heterogeneous pattern of green fluorescence was detected in infected cells, from a diffuse staining (likely corresponding to unassembled Gag proteins) to strong signals at the cell surface (see Movie S2 in the supplemental material). We observed infected cells associated with one or more targets, and contacts were rather stable over the analysis period. In some clusters, polysynapse-like structures were readily visible, with a concomitant polarization of Gag toward multiple junctions and fluorescent dots eventually reaching target cells. Frame-by-frame time-lapse analysis of one representative sequence (see Movie S2a in the supplemental material) suggested that Gag proteins were moving at the plasma membrane to gain access to the junction (Fig. 4d). In other cases, the Gag signal progressively accumulated at the contact zone, without previous detectable movement at the surface (see Movie S2 in the supplemental material). In addition, Gag spots moving on filopodia-like structures were visible, whereas in other cells, the surface signal was not engaged with recipients (see Movie S2 in the supplemental material). Altogether, real-time analysis confirmed that diverse modes of Gag movements and transfer occur in infected lymphocytes. Polysynapses are likely generated by a simultaneous budding of virions toward the junctions, as well as by a rapid movement of viral proteins or particles at the cell surface.

In cultures of HIV-infected monocyte-derived DCs mixed

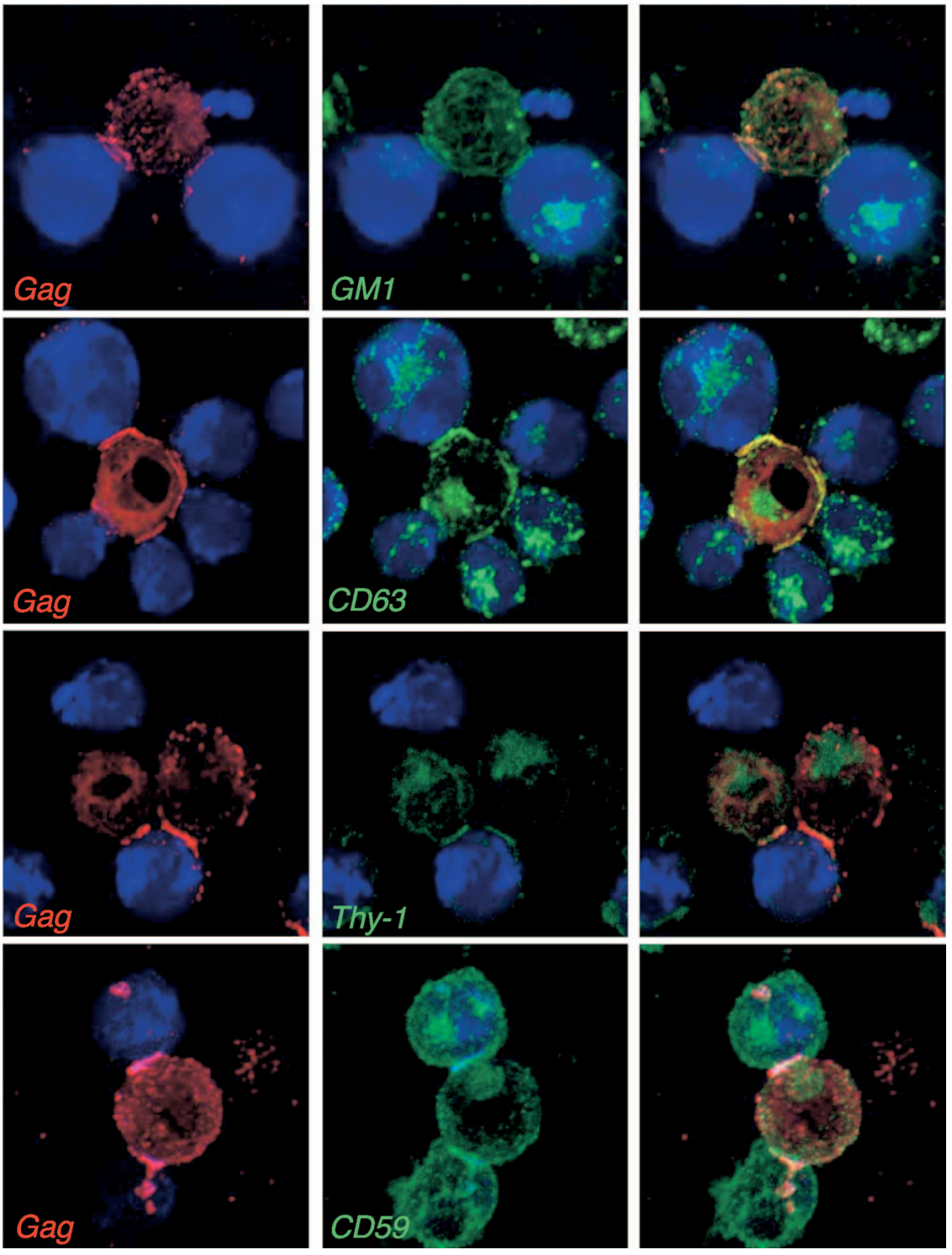

FIG. 3. Localization of cellular molecules in virological polysynapses. Conjugates between infected cells and targets (blue) were stained with anti-Gag (red) and with either the GM1 raft marker, anti-CD63, anti-Thy-1, or anti-CD59 MAbs. Representative images of polysynapses from at least three independent experiments are shown. Right panels are merged images of the left and middle panels.

with lymphocytes, we observed single donors engaged with multiple targets (see Fig. S3b in the supplemental material). In these clusters, Gag proteins simultaneously accumulated at multiple sites of junction. Therefore, polysynapses readily form in other immune cells susceptible to HIV-1 infection. This mechanism of viral spreading thus seems to be quite general.

Regulation of HIV replication and polysynapse formation by LFA-1. The contribution of adhesion molecules such as LFA-1

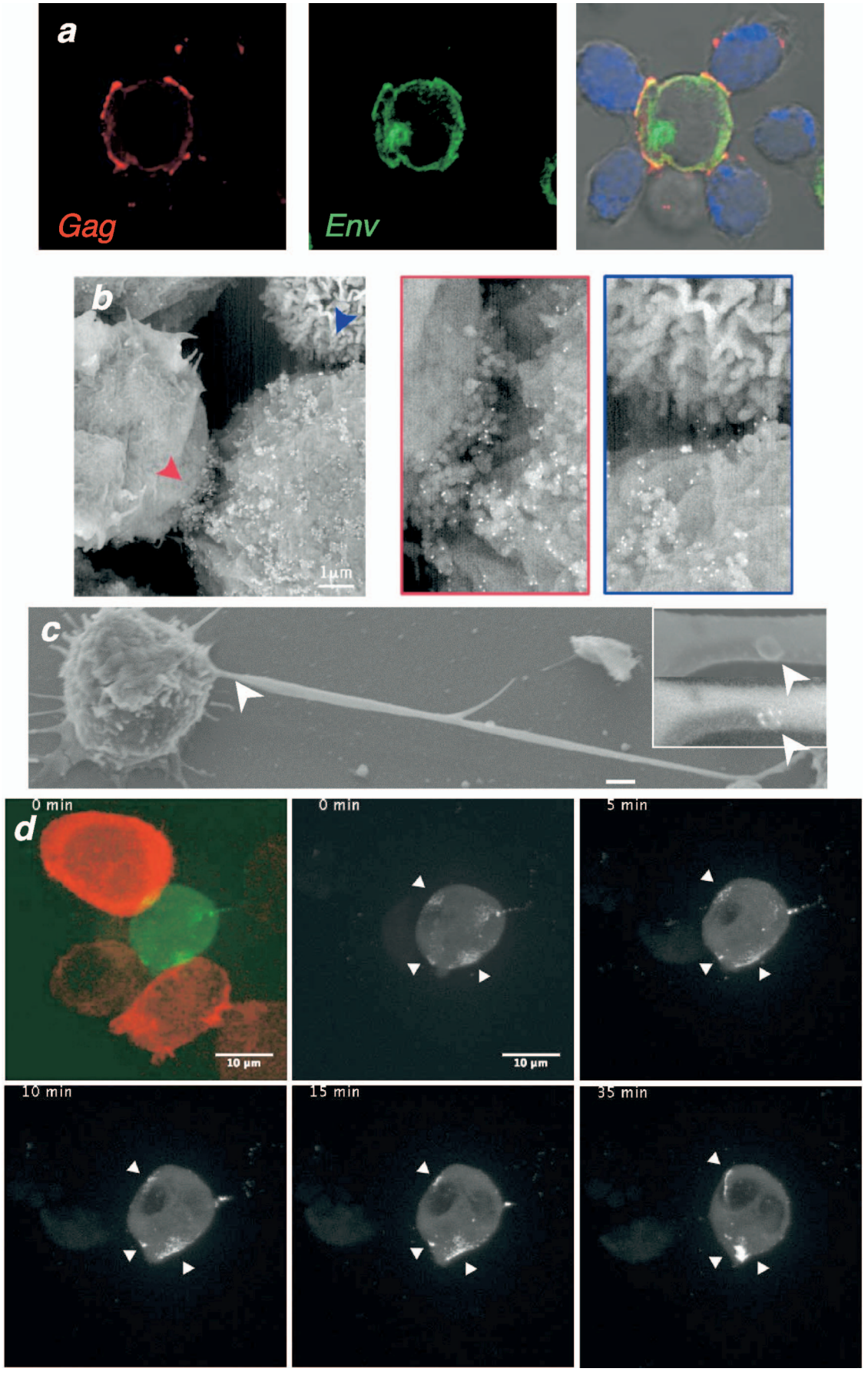
a
Gag
Env
b
1μm
c
d
0 min
10 μm
0 min
10 μm
5 min
10 min
15 min
35 min

to HIV replication and cell-to-cell transfer has been broadly studied, with variable conclusions. It was initially suggested that LFA-1 is required for syncytium formation but not for HIV replication (40). However, the conformational state, and hence the affinity of LFA-1 to its ligand ICAM-1, modulates susceptibility to HIV infection (9, 15, 51). Some recent reports demonstrated that the adhesion molecules LFA-1, ICAM-1, and ICAM-3 facilitate VS formation between T cells (2, 23), although viral transfer may occur even in the absence of LFA-1 (42). We thus assessed the impact of LFA-1 on HIV replication and polysynapse formation.

To this end, we used Jβ2.7 cells, a Jurkat derivative lacking LFA-1 due to the absence of the α chain (CD11a), and Jβ2.7-LFA-1$^+$ cells, in which expression of the integrin was restored by transfection (15). Both cell lines expressed similar levels of CD4 and CXCR4 coreceptors (not shown). Cells were infected at two multiplicities of infection (MOI) and HIV replication was assessed by measuring the appearance of Gag$^+$ cells over time. As previously reported (15), viral replication was delayed in Jβ2.7 cells compared to that in Jβ2.7-LFA-1$^+$ cells (Fig. 6a). This impairment was more visible at a low MOI. In four independent experiments, in cells expressing the integrin, the percentage of Gag$^+$ cells, at days 6 to 10 postinfection, was two- to threefold higher than those measured in LFA-1-deficient cells (Fig. 6a).

We then investigated the impact of LFA-1 on cell-to-cell HIV transfer using a quantitative flow cytometry-based assay (48). HIV-infected Jβ2.7 and Jβ2.7-LFA-1$^+$ cells (25% Gag$^+$ cells in both cell types) were used as donors and incubated with CFSE-stained wild-type Jurkat recipients. Viral infection was then followed by measuring Gag levels in targets at different times (Fig. 6b). As expected, LFA-1$^+$ cells efficiently transmitted HIV to targets, with about 25% and 35% of Gag$^+$ cells at 24 h and 48 h post-coculture, respectively. LFA-1-deficient cells less potently transmitted HIV, with about 10% and 20% Gag$^+$ cells at 24 h and 48 h of coculture (Fig. 6b). In three independent experiments, there was a 40% decrease in the efficiency of viral transfer from LFA-1-defective cells (Fig. 6b).

We next asked whether LFA-1 impacts the engagement of Gag proteins at junctions between donors and recipients. HIV-infected Jβ2.7 and Jβ2.7-LFA-1$^+$ cells were incubated for 1 h with Far Red dye-labeled Jurkat recipients, and single and multiple conjugates with Gag polarization were scored. Interestingly, in the absence of the integrin, the Gag staining was less clustered at cell interfaces. There was a 60% decrease in the number of cells displaying Gag polarization and engaged in either single or multiple conjugates (Fig. 6c). Altogether, these data show that the absence of LFA-1 impairs HIV replication, cell-to-cell transfer, and formation of single VS and polysynapses.

Visualization of clusters of SIV-infected cells in vivo. We then examined interactions between SIV-producing (SIV RNA$^+$) cells in macaque tissues, at the acute phase of infection (day 12 post-vaginal inoculation), using a sensitive in situ hybridization method (54) that enables visualization of SIV RNA both in cells and virions produced by these cells. We observed, both in the ectocervical submucosa (Fig. 7a) and in the T-cell zone of an axillary lymph node (Fig. 7b), not only the previously described individual small and large "resting" and activated infected CD4$^+$ T cells (54) but also small clusters of two to four infected cells in cervix, and in lymph node large clusters of as many as 12 SIV RNA$^+$ cells. These in vivo experiments do not allow us to conclusively determine whether the clustering is due to multiple rounds of monosynapses or to polysynapses. Therefore, these clusters in snapshots of infection do not formally prove that polysynapses are operative in the infected host but strongly suggest that one infected cell may simultaneously transmit the infection to multiple targets.

DISCUSSION

Here, we provide a global view of the diverse modes of HIV cell-to-cell transfer. Quantitative analysis indicated that single synapses, polysynapses, and thin membrane protrusions mediate viral spread in lymphocytes. Close interactions between infected and target cells, leading to a polarization of HIV Gag proteins at the contact zone, were frequently observed (25% and 15 to 20% of infected cells engaged in single and polysynapses, respectively). Filopodial bridges (46) and nanotube-like structures (50) transporting HIV-1 material were less frequent (<10% of infected cells), at least in our experimental setting, but may promote viral transfer to targets that are not in the immediate vicinity of infected cells. We show that HIV (in part through Env expression) manipulates cell-cell interactions and enhances these three types of contacts.

We identified a mechanism by which HIV-1 spreads in cultures from one infected cell to multiple (two to six) recipients, through polysynapses. These rosette-like structures, displaying multifocal Gag accumulation, were observed in infected lymphocytes and DCs. That Env-expressing cells can enter in contact with several cells was not unexpected. Images illustrating these multiple contacts appear sometimes in the literature (46, 50), but this phenomenon has not been the subject of a detailed investigation. The classical VS, initially described for HTLV-1 (20), corresponds to a single donor engaging a single recipient, with a polarization of the MTOC and viral budding toward the site of contact. Obviously, this model cannot apply to HIV polysynapses, which require a more flexible mode of formation. Rather, because GM1, as well as CD63, Thy-1, and CD59 frequently colocalized with HIV-1 Gag at the sites of

FIG. 4. HIV budding and accumulation at the sites of cell-cell connections. (a) Localization of Gag (red) and Env (green) viral proteins in virological polysynapses, analyzed as described in the legend to Fig. 1. (b and c) SEM views of HIV-infected Jurkat cells (b) or primary CD4$^+$ cells (c) mixed with uninfected cells for 1 h. HIV-1 virions are stained with anti-Env MAb coupled to gold particles (appearing as white dots). Representative images of polysynapses (b) and of long cellular protrusions carrying Env$^+$ virus-like particles (c) are depicted. The regions pointed at by arrows in the left panels are magnified in the right boxes. In panel c, the inserts illustrate a virus-like particle (upper panel), with a compact Env signal (lower panel). (d) Real-time imaging of Gag movements toward two targets. The infected cell (green) carries an HIV Gag.eGFP virus. The two target cells are stained in red (left panel). Gag movements are analyzed at the indicated time points. Images are snapshots from Movie S2 in the supplemental material. The arrows indicate zones of intercellular contacts.

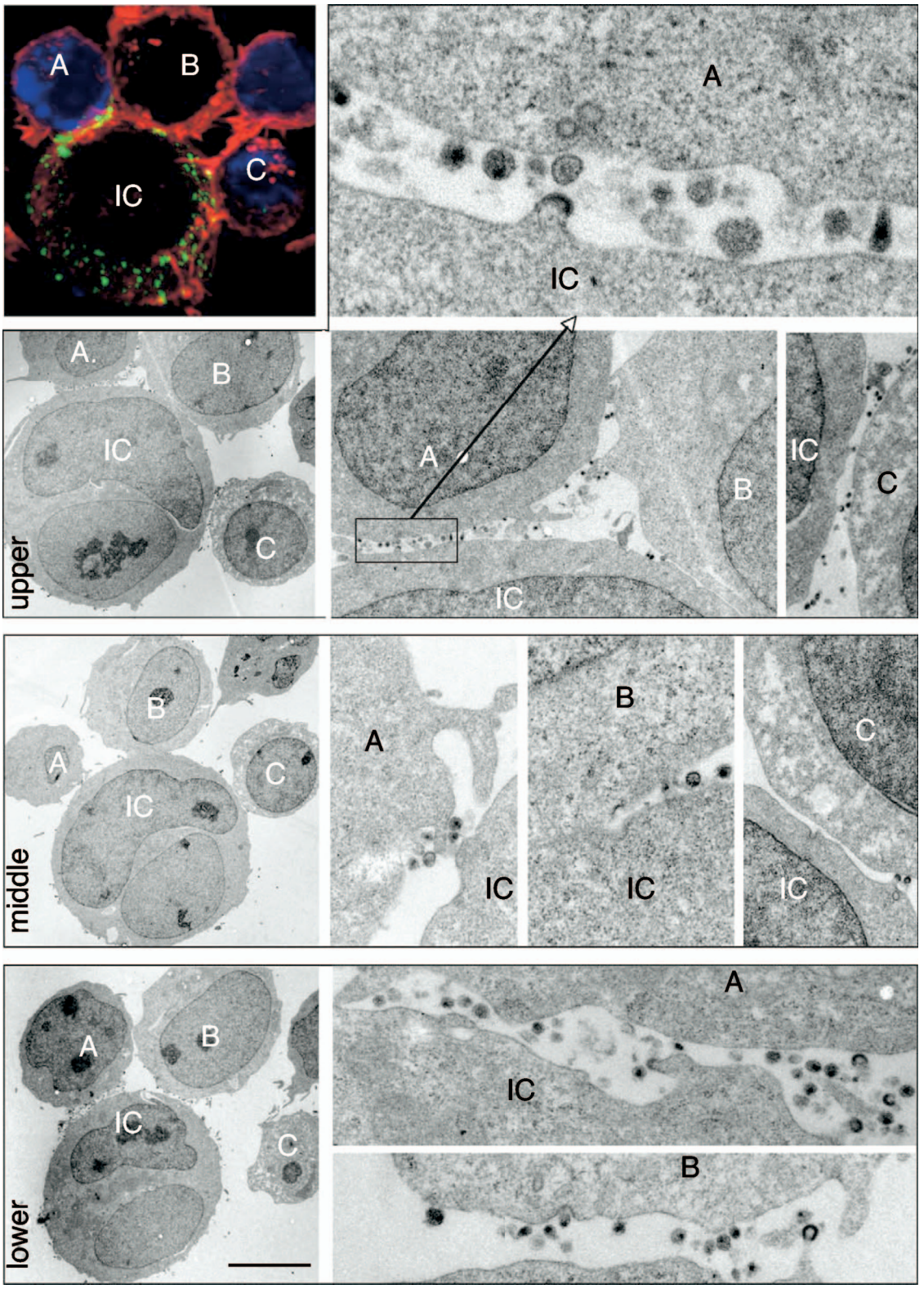

FIG. 5. Analysis of polysynapses by correlative IF-TEM. HIV-1-infected Jurkat cells were mixed with Far Red dye-labeled Jurkat recipients (blue) for 1 h and stained for HIV-1 Gag (green) and F-actin (red). Samples were placed on a grid with a coordinate system to locate the regions of interest. In the upper left panel, a conjugate formed between one infected cell (IC) and three target cells (labeled A, B, and C) is visualized by confocal microscopy. Samples were then sectioned, and the same conjugate was analyzed by TEM. Three sections, at 0.5 to 1-μm intervals (*z* axis), are depicted on the three lower left panels. They correspond approximately to the upper, middle, and lower regions of the conjugate. Various magnifications of the intercellular contact zones are depicted in the right panels. The scale bar represents 5 μm.

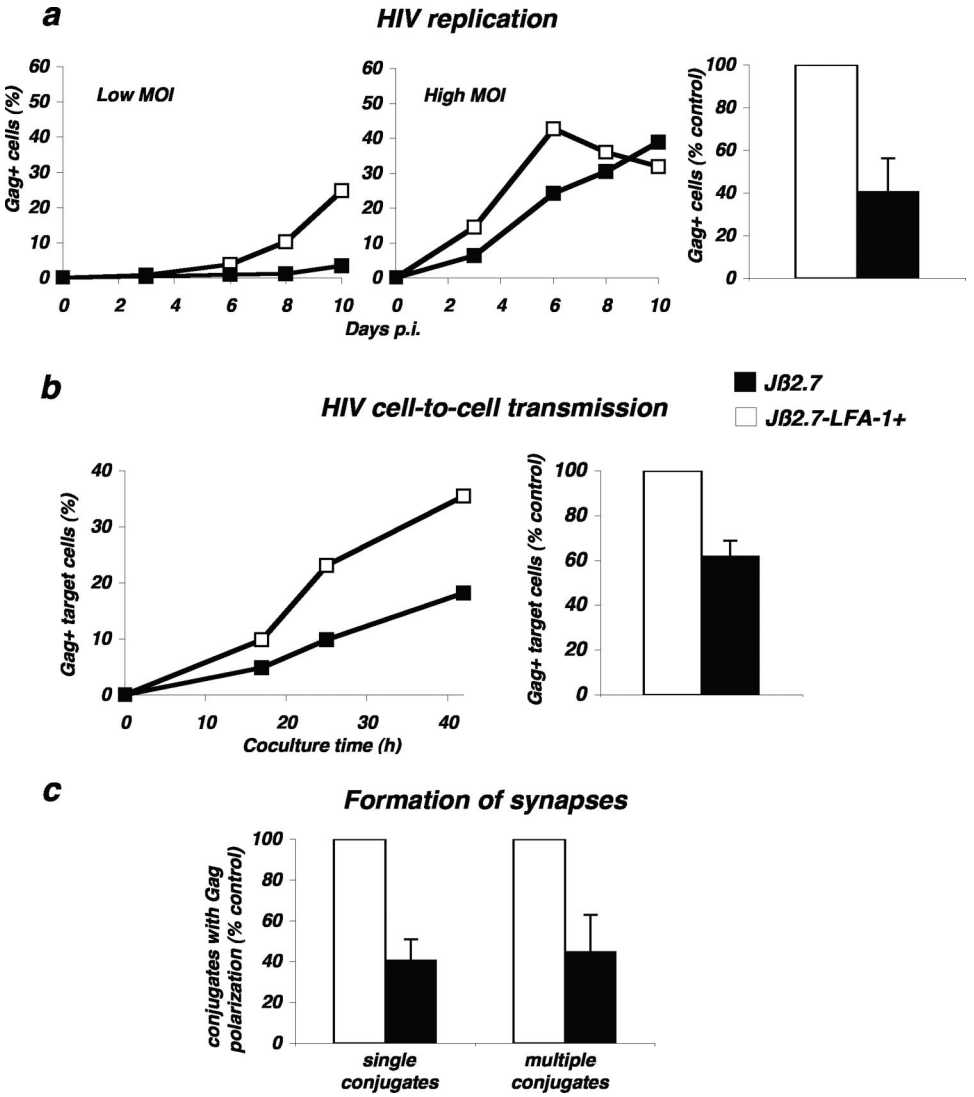

FIG. 6. Role of LFA-1 during HIV replication and cell-to-cell transfer. (a) HIV replication is impaired in LFA-1-defective Jurkat cells. Cells of the Jurkat derivative Jβ2.7 (which lacks LFA-1) and Jβ2.7-LFA-1$^+$ cells were exposed to HIV (NL4-3 strain), at either a low (5 ng/10^6 cells/ml) or high (50 ng/10^6 cells/ml) MOI. Viral replication was followed by measuring the percentage of Gag$^+$ cells by flow cytometry at the indicated days postinfection (p.i.). A representative experiment is shown in the left panel. The mean ± standard deviation of three independent experiments is depicted in the right panel, with 100% corresponding to values obtained in Jβ2.7-LFA1$^+$ cells at the peak at all MOIs. (b) HIV cell-to-cell transfer analyzed by flow cytometry. Productively HIV-infected Jβ2.7-LFA1$^+$ and Jβ2.7 cells (about 25% Gag$^+$) were cocultivated with target CFSE$^+$ Jurkat cells at a 1/10 ratio. The percentage of Gag$^+$ cells among targets (CFSE$^+$) is shown at the indicated times of coculture. A representative experiment is shown on the left. The mean ± standard deviation of four independent experiments (16-h time point, with the donor/recipient ratio varying from 1/3 to 1/10) is depicted in the right panel, with 100% corresponding to values obtained in Jβ2.7-LFA1$^+$ cells. (c) Formation of single VS and polysynapses. Productively HIV-infected Jβ2.7-LFA1$^+$ and Jβ2.7 cells (about 25 to 40% Gag$^+$) were cocultivated for 1 h with the target Far Red dye-labeled Jurkat cells. Single and multiple conjugates displaying Gag clustering at the junction zone with targets were scored. Data are means ± standard deviations of four independent experiments, with 100% corresponding to values obtained in Jβ2.7-LFA1$^+$ cells (with totals of 535 Jβ2.7-LFA1$^+$ and 592 Jβ2.7-infected cells analyzed).

contacts, it is likely that the multifocal capping of assembled or budding virions required for polysynapse formation is promoted by tetraspanins and plasma membrane mobility via lipid rafts. Released HIV-1 particles incorporate various cellular molecules, including GM1, Thy-1, and CD59 (38), implicating rafts as platforms of HIV budding (30, 31, 39). Our results extend these observations and highlight a major role for rafts in polysynapse formation. The involvement of lipid rafts was further supported by our observation that cholesterol depletion of infected cells with β-methyl-cyclodextrin strongly inhibited both cell contacts and Gag polarization in polysynapses (not shown). Actin and microtubules are also likely involved in transporting Gag proteins toward the plasma membrane or in movement of surface viral proteins or particles toward polysynapses, because nocodazole, cytochalasin D, and latrunculin B inhibited polysynapse formation. It is well documented that retroviruses have evolved means to hijack actin as well as microtubule skeletal networks to traffic (8, 37). Whether the

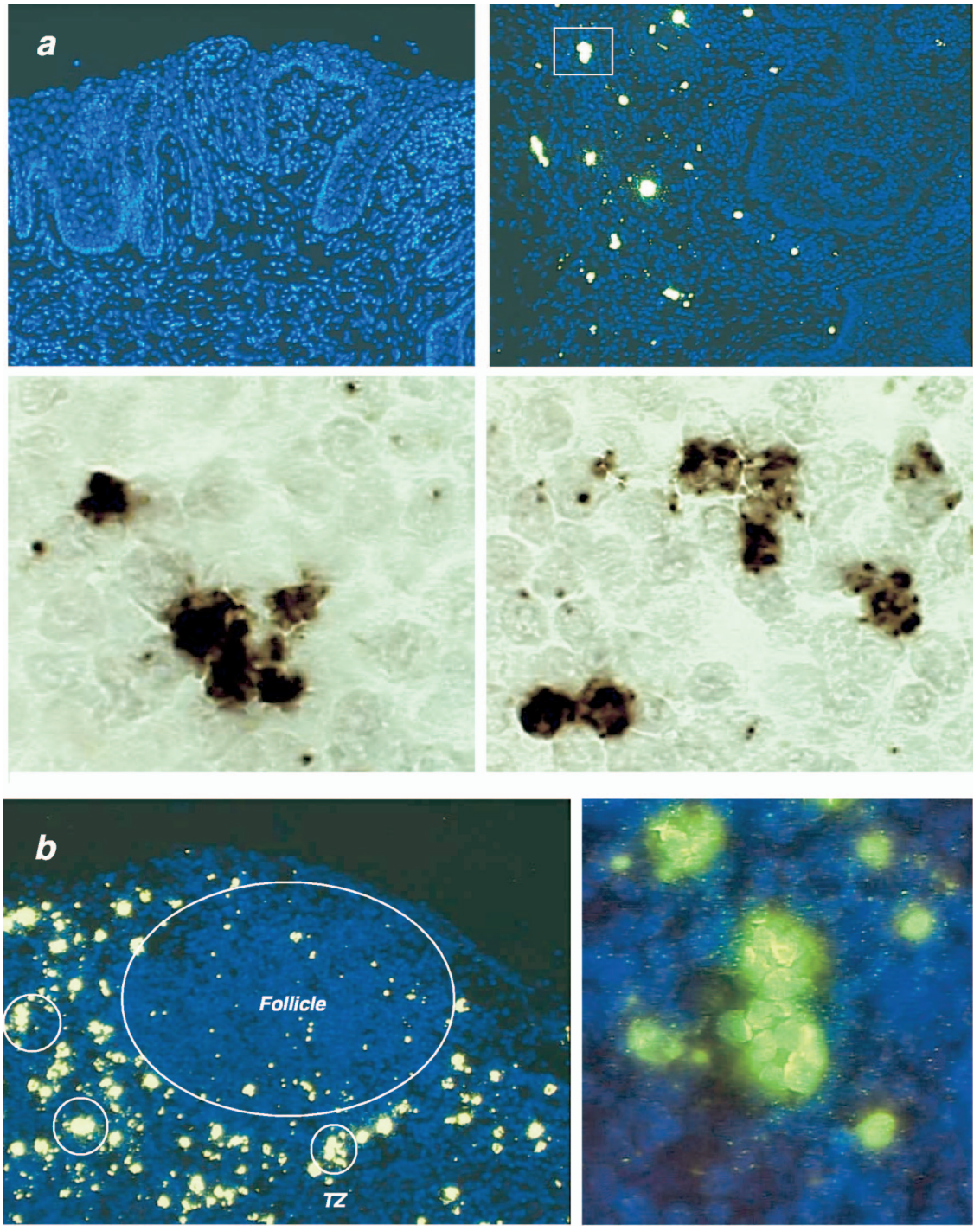

FIG. 7. Detection of clusters of infected cells in macaque tissues 12 days after vaginal inoculation of SIV. SIV RNA was detected by in situ hybridization and tyramide signal amplification with subsequent staining with fluorescent ELF (enzyme-labeled fluorescence; yellow signal) or DAB (3,3′-diaminobenzidine; brown signal) substrates. (a) Analysis of the ectocervix. (Upper left panel) Hybridization with a sense probe as a negative control; (upper right panel), antisense probe, detection of SIV RNA$^+$ large activated and smaller "resting" CD4 T cells, and clusters of infected cells (one such cluster is enclosed by rectangle). At higher magnification (lower panels), the clusters consist of two to six SIV RNA$^+$ cells. (b) Analysis of an axillary lymph node. The follicle and T-cell zone (TZ) are indicated on the left panel. Clusters of infected cells in the TZ are encircled. (Right panel) Clusters at higher magnification.

cytoskeleton provides concomitant routes of HIV transport to various regions of the surface or oscillates toward the different target cells will require further investigation. However, our combined use of IF, correlative microscopy, and time-lapse imaging strongly suggests that the multiple viral transfer zones of polysynapses can be formed simultaneously, rather than one after another.

In the immune synapse formed between one cytotoxic T

lymphocyte (CTL) and its target, the MTOC is drawn vectorially to the contact site by a microtubule sliding mechanism and then oscillates laterally (29). Thus, highly dynamic movements of the cytoskeleton likely promote formation of virological polysynapses. Assembly of individual virions at the plasma membrane is a rapid phenomenon (5 min) (27). A fast viral assembly may be instrumental for polysynapse formation.

It is noteworthy that we report here a supramolecular structure of Gag proteins which accumulate in a ring-shaped zone at the junctions. This structure was observed in VS as well as in polysynapses and resembles the pSMAC of adhesion molecules in the immune synapse (6, 29). We report here that LFA-1, an integrin previously known to facilitate HIV replication, also enhances cell-to-cell viral transfer and formation of single synapses and polysynapses. Whether other adhesion molecules, like ICAM-1 (52), and whether the recently described HIV-1 Env-$\alpha 4\beta 7$ integrin interaction (2) stabilize Gag rings and polysynapses remain to be determined. It will be also worth examining the role of viral accessory proteins (32) as well as that of the MVB-associated HIV budding machinery (35) in formation of Gag rings and polysynapses. Interestingly, a central clustering of Env was documented, in a situation where this viral protein is situated in planar bilayers that contact uninfected T cells (52). Furthermore, quantitative 3D videomicroscopy revealed the formation of micrometer-sized "buttons" of Gag at the junction zones of infected Jurkat cells and primary CD4 T cells (18). The links that may exist between the topology of Env proteins and of Gag rings and/or buttons will deserve further investigation.

Viruses exploit the normal physiology of cells to spread. The identification of virological polysynapses suggests that immune cells may simultaneously exchange signals and information with multiple adjacent cells. Examples of such functional multiple contacts are scarce. For instance, CD4 T cells can integrate signals from multiple antigen-presenting cells simultaneously (4), whereas cytotoxic T lymphocytes polarize lytic granules toward different cells and may kill more than one target at a time (19, 29, 53). Polysynapses likely represent an underestimated mode of communication in immune cells, and it will be of interest to investigate the role of signaling events (48) in the establishment of virological polysynapses.

In lymphoid and mucosal tissues, a high cell density and a low speed of lymphocytes (10 μm/min) allow multiple encounters between cells. That clusters of infected cells are detected in such tissues suggests that virological polysynapses are biologically relevant. Polysynapses could play a critical role in the exponential explosive propagation that characterizes the acute phase of infection (14, 16). It is also tempting to speculate that polysynapses, by enhancing locally the MOI, provide a means for HIV and other viruses to escape innate, intrinsic, and adaptative immune responses (32).

ACKNOWLEDGMENTS

We thank Matthew Albert, Philippe Bousso, Jean-Michel Heard, and members of the Virus and Immunity Unit for support, discussions, and critical reading of the manuscript; Christophe Machu, Pascal Roux, Emmanuel Perret, and Spencer Shorte (Institut Pasteur Imagopole) for support with image and film acquisition; Nadège Cayet for electron microscopy analysis; Anna Sartori for help with correlative IF-TEM analysis; Jean-Marc Panaud for movie cutting; and Barbara Muller, Catarina Hioe, Claire Hivroz, and the NIH AIDS Research and Reference Reagent Program for the kind gift of reagents.

This work was supported by grants from Agence Nationale de Recherche sur le SIDA (ANRS), Sidaction, CNRS, Fondation de France, European Community (FP7 contract no. 201412), and Institut Pasteur. D.R. is supported by a Marie Curie fellowship (FP6 contract, INTRAPATH program).

REFERENCES

1. **Alfsen, A., H. Yu, A. Magerus-Chatinet, A. Schmitt, and M. Bomsel.** 2005. HIV-1-infected blood mononuclear cells form an integrin- and agrin-dependent viral synapse to induce efficient HIV-1 transcytosis across epithelial cell monolayer. Mol. Biol. Cell **16:**4267–4279.
2. **Arthos, J., C. Cicala, E. Martinelli, K. Macleod, D. Van Ryk, D. Wei, Z. Xiao, T. D. Veenstra, T. P. Conrad, R. A. Lempicki, S. McLaughlin, M. Pascuccio, R. Gopaul, J. McNally, C. C. Cruz, N. Censoplano, E. Chung, K. N. Reitano, S. Kottilil, D. J. Goode, and A. S. Fauci.** 2008. HIV-1 envelope protein binds to and signals through integrin alpha4beta7, the gut mucosal homing receptor for peripheral T cells. Nat. Immunol. **9:**301–309.
3. **Chen, P., W. Hübner, M. A. Spinelli, and B. K. Chen.** 2007. Predominant mode of human immunodeficiency virus transfer between T cells is mediated by sustained Env-dependent neutralization-resistant virological synapses. J. Virol. **81:**12582–12595.
4. **Depoil, D., R. Zaru, M. Guiraud, A. Chauveau, J. Harriague, G. Bismuth, C. Utzny, S. Muller, and S. Valitutti.** 2005. Immunological synapses are versatile structures enabling selective T cell polarization. Immunity **22:**185–194.
5. **Dixit, R., V. Tiwari, and D. Shukla.** 2008. Herpes simplex virus type 1 induces filopodia in differentiated P19 neural cells to facilitate viral spread. Neurosci. Lett. **440:**113–118.
6. **Dustin, M. L.** 2007. Cell adhesion molecules and actin cytoskeleton at immune synapses and kinapses. Curr. Opin. Cell Biol. **19:**529–533.
7. **Eugenin, E. A., P. J. Gaskill, and J. W. Berman.** 2009. Tunneling nanotubes (TNT) are induced by HIV-infection of macrophages: a potential mechanism for intercellular HIV trafficking. Cell. Immunol. **254:**142–148.
8. **Fackler, O. T., and H. G. Krausslich.** 2006. Interactions of human retroviruses with the host cell cytoskeleton. Curr. Opin. Microbiol. **9:**409–415.
9. **Fortin, J. F., B. Barbeau, H. Hedman, E. Lundgren, and M. J. Tremblay.** 1999. Role of the leukocyte function antigen-1 conformational state in the process of human immunodeficiency virus type 1-mediated syncytium formation and virus infection. Virology **257:**228–238.
10. **Garcia, E., M. Pion, A. Pelchen-Matthews, L. Collinson, J. F. Arrighi, G. Blot, F. Leuba, J. M. Escola, N. Demaurex, M. Marsh, and V. Piguet.** 2005. HIV-1 trafficking to the dendritic cell-T-cell infectious synapse uses a pathway of tetraspanin sorting to the immunological synapse. Traffic **6:**488–501.
11. **Gousset, K., S. D. Ablan, L. V. Coren, A. Ono, F. Soheilian, K. Nagashima, D. E. Ott, and E. O. Freed.** 2008. Real-time visualization of HIV-1 GAG trafficking in infected macrophages. PLoS Pathog. **4:**e1000015.
12. **Gratton, S., R. Cheynier, M. J. Dumaurier, E. Oksenhendler, and S. Wain-Hobson.** 2000. Highly restricted spread of HIV-1 and multiply infected cells within splenic germinal centers. Proc. Natl. Acad. Sci. USA **97:**14566–14571.
13. **Groot, F., S. Welsch, and Q. J. Sattentau.** 2008. Efficient HIV-1 transmission from macrophages to T cells across transient virological synapses. Blood **111:**4660–4663.
14. **Haase, A. T.** 2005. Perils at mucosal front lines for HIV and SIV and their hosts. Nat. Rev. Immunol. **5:**783–792.
15. **Hioe, C. E., P. C. Chien, Jr., C. Lu, T. A. Springer, X.-H. Wang, J. Bandres, and M. Tuen.** 2001. LFA-1 expression on target cells promotes human immunodeficiency virus type 1 infection and transmission. J. Virol. **75:**1077–1082.
16. **Hladik, F., and M. J. McElrath.** 2008. Setting the stage: host invasion by HIV. Nat. Rev. Immunol. **8:**447–457.
17. **Hope, T. J.** 2007. Bridging efficient viral infection. Nat. Cell Biol. **9:**243–244.
18. **Hubner, W., G. P. McNerney, P. Chen, B. M. Dale, R. E. Gordon, F. Y. Chuang, X. D. Li, D. M. Asmuth, T. Huser, and B. K. Chen.** 2009. Quantitative 3D video microscopy of HIV transfer across T cell virological synapses. Science **323:**1743–1747.
19. **Huppa, J. B., and M. M. Davis.** 2003. T-cell-antigen recognition and the immunological synapse. Nat. Rev. Immunol. **3:**973–983.
20. **Igakura, T., J. C. Stinchcombe, P. K. Goon, G. P. Taylor, J. N. Weber, G. M. Griffiths, Y. Tanaka, M. Osame, and C. R. Bangham.** 2003. Spread of HTLV-I between lymphocytes by virus-induced polarization of the cytoskeleton. Science **299:**1713–1716.
21. **Izquierdo-Useros, N., M. Naranjo-Gomez, J. Archer, S. C. Hatch, I. Erkizia, J. Blanco, F. E. Borras, M. C. Puertas, J. H. Connor, M. T. Fernandez-Figueras, L. Moore, B. Clotet, S. Gummuluru, and J. Martinez-Picado.** 2009. Capture and transfer of HIV-1 particles by mature dendritic cells converges with the exosome-dissemination pathway. Blood **113:**2732–2741.
22. **Jolly, C., K. Kashefi, M. Hollinshead, and Q. J. Sattentau.** 2004. HIV-1 cell to cell transfer across an Env-induced, actin-dependent synapse. J. Exp. Med. **199:**283–293.
23. **Jolly, C., I. Mitar, and Q. J. Sattentau.** 2007. Adhesion molecule interactions

facilitate human immunodeficiency virus type 1-induced virological synapse formation between T cells. J. Virol. **81:**13916–13921.
24. **Jolly, C., I. Mitar, and Q. J. Sattentau.** 2007. Requirement for an intact T-cell actin and tubulin cytoskeleton for efficient assembly and spread of human immunodeficiency virus type 1. J. Virol. **81:**5547–5560.
25. **Jolly, C., and Q. J. Sattentau.** 2007. Human immunodeficiency virus type 1 assembly, budding, and cell-cell spread in T cells take place in tetraspanin-enriched plasma membrane domains. J. Virol. **81:**7873–7884.
26. **Jolly, C., and Q. J. Sattentau.** 2005. Human immunodeficiency virus type 1 virological synapse formation in T cells requires lipid raft integrity. J. Virol. **79:**12088–12094.
27. **Jouvenet, N., P. D. Bieniasz, and S. M. Simon.** 2008. Imaging the biogenesis of individual HIV-1 virions in live cells. Nature **454:**236–240.
28. **Jouvenet, N., M. Windsor, J. Rietdorf, P. Hawes, P. Monaghan, M. Way, and T. Wileman.** 2006. African swine fever virus induces filopodia-like projections at the plasma membrane. Cell. Microbiol. **8:**1803–1811.
29. **Kuhn, J. R., and M. Poenie.** 2002. Dynamic polarization of the microtubule cytoskeleton during CTL-mediated killing. Immunity **16:**111–121.
30. **Leung, K., J. O. Kim, L. Ganesh, J. Kabat, O. Schwartz, and G. J. Nabel.** 2008. HIV-1 assembly: viral glycoproteins segregate quantally to lipid rafts that associate individually with HIV-1 capsids and virions. Cell Host Microbe **3:**285–292.
31. **Lindwasser, O. W., and M. D. Resh.** 2001. Multimerization of human immunodeficiency virus type 1 Gag promotes its localization to barges, raft-like membrane microdomains. J. Virol. **75:**7913–7924.
32. **Malim, M. H., and M. Emerman.** 2008. HIV-1 accessory proteins—ensuring viral survival in a hostile environment. Cell Host Microbe **3:**388–398.
33. **McDonald, D., L. Wu, S. M. Bohks, V. N. KewalRamani, D. Unutmaz, and T. J. Hope.** 2003. Recruitment of HIV and its receptors to dendritic cell-T cell junctions. Science **300:**1295–1297.
34. **Mercer, J., and A. Helenius.** 2008. Vaccinia virus uses macropinocytosis and apoptotic mimicry to enter host cells. Science **320:**531–535.
35. **Morita, E., and W. I. Sundquist.** 2004. Retrovirus budding. Annu. Rev. Cell Dev. Biol. **20:**395–425.
36. **Muller, B., J. Daecke, O. T. Fackler, M. T. Dittmar, H. Zentgraf, and H. G. Krausslich.** 2004. Construction and characterization of a fluorescently labeled infectious human immunodeficiency virus type 1 derivative. J. Virol. **78:**10803–10813.
37. **Naghavi, M. H., and S. P. Goff.** 2007. Retroviral proteins that interact with the host cell cytoskeleton. Curr. Opin. Immunol. **19:**402–407.
38. **Nguyen, D. H., and J. E. K. Hildreth.** 2000. Evidence for budding of human immunodeficiency virus type 1 selectively from glycolipid-enriched membrane lipid rafts. J. Virol. **74:**3264–3272.
39. **Ono, A., and E. O. Freed.** 2001. Plasma membrane rafts play a critical role in HIV-1 assembly and release. Proc. Natl. Acad. Sci. USA **98:**13925–13930.
40. **Pantaleo, G., L. Butini, C. Graziosi, G. Poli, S. M. Schnittman, J. J. Greenhouse, J. I. Gallin, and A. S. Fauci.** 1991. Human immunodeficiency virus (HIV) infection in CD4+ T lymphocytes genetically deficient in LFA-1: LFA-1 is required for HIV-mediated cell fusion but not for viral transmission. J. Exp. Med. **173:**511–514.
41. **Phillips, D. M.** 1994. The role of cell-to-cell transmission in HIV infection. AIDS **8:**719–731.
42. **Puigdomenech, I., M. Massanella, N. Izquierdo-Useros, R. Ruiz-Hernandez, M. Curriu, M. Bofill, J. Martinez-Picado, M. Juan, B. Clotet, and J. Blanco.** 2008. HIV transfer between CD4 T cells does not require LFA-1 binding to ICAM-1 and is governed by the interaction of HIV envelope glycoprotein with CD4. Retrovirology **5:**32.
43. **Ruggiero, E., R. Bona, C. Muratori, and M. Federico.** 2008. Virological consequences of early events following cell-cell contact between human immunodeficiency virus type 1-infected and uninfected $CD4^+$ cells. J. Virol. **82:**7773–7789.
44. **Sattentau, Q.** 2008. Avoiding the void: cell-to-cell spread of human viruses. Nat. Rev. Microbiol. **6:**815–826.
45. **Schelhaas, M., H. Ewers, M. L. Rajamaki, P. M. Day, J. T. Schiller, and A. Helenius.** 2008. Human papillomavirus type 16 entry: retrograde cell surface transport along actin-rich protrusions. PLoS Pathog. **4:**e1000148.
46. **Sherer, N. M., M. J. Lehmann, L. F. Jimenez-Soto, C. Horensavitz, M. Pypaert, and W. Mothes.** 2007. Retroviruses can establish filopodial bridges for efficient cell-to-cell transmission. Nat. Cell Biol. **9:**310–315.
47. **Sherer, N. M., and W. Mothes.** 2008. Cytonemes and tunneling nanotubules in cell-cell communication and viral pathogenesis. Trends Cell Biol. **18:**414–420.
48. **Sol-Foulon, N., M. Sourisseau, F. Porrot, M. I. Thoulouze, C. Trouillet, C. Nobile, F. Blanchet, V. di Bartolo, N. Noraz, N. Taylor, A. Alcover, C. Hivroz, and O. Schwartz.** 2007. ZAP-70 kinase regulates HIV cell-to-cell spread and virological synapse formation. EMBO J. **26:**516–526.
49. **Sourisseau, M., N. Sol-Foulon, F. Porrot, F. Blanchet, and O. Schwartz.** 2007. Inefficient human immunodeficiency virus replication in mobile lymphocytes. J. Virol. **81:**1000–1012.
50. **Sowinski, S., C. Jolly, O. Berninghausen, M. A. Purbhoo, A. Chauveau, K. Kohler, S. Oddos, P. Eissmann, F. M. Brodsky, C. Hopkins, B. Onfelt, Q. Sattentau, and D. M. Davis.** 2008. Membrane nanotubes physically connect T cells over long distances presenting a novel route for HIV-1 transmission. Nat. Cell Biol. **10:**211–219.
51. **Tardif, M. R., and M. J. Tremblay.** 2005. Regulation of LFA-1 activity through cytoskeleton remodeling and signaling components modulates the efficiency of HIV type-1 entry in activated CD4+ T lymphocytes. J. Immunol. **175:**926–935.
52. **Vasiliver-Shamis, G., M. Tuen, T. W. Wu, T. Starr, T. O. Cameron, R. Thomson, G. Kaur, J. Liu, M. L. Visciano, H. Li, R. Kumar, R. Ansari, D. P. Han, M. W. Cho, M. L. Dustin, and C. E. Hioe.** 2008. Human immunodeficiency virus type 1 envelope gp120 induces a stop signal and virological synapse formation in noninfected $CD4^+$ T cells. J. Virol. **82:**9445–9457.
53. **Wiedemann, A., D. Depoil, M. Faroudi, and S. Valitutti.** 2006. Cytotoxic T lymphocytes kill multiple targets simultaneously via spatiotemporal uncoupling of lytic and stimulatory synapses. Proc. Natl. Acad. Sci. USA **103:**10985–10990.
54. **Zhang, Z. Q., S. W. Wietgrefe, Q. Li, M. D. Shore, L. Duan, C. Reilly, J. D. Lifson, and A. T. Haase.** 2004. Roles of substrate availability and infection of resting and activated CD4+ T cells in transmission and acute simian immunodeficiency virus infection. Proc. Natl. Acad. Sci. USA **101:**5640–5645.